

-Supporting Information

Site-Directed Synthesis of Cobalt Oxide Clusters in a Metal–Organic Framework

Aaron W. Peters,¹ Kenichi Otake,¹ Ana E. Platero-Prats,^{2†} Zhanyong Li,¹ Matthew R. DeStefano,¹ Karena W. Chapman,² Omar K. Farha,^{1,3*} and Joseph T. Hupp^{1*}

¹*Department of Chemistry, Northwestern University, 2145 Sheridan Road, Evanston, Illinois 60208, United States*

²*X-ray Science Division, Advanced Photon Source, Argonne National Laboratory, Argonne, Illinois 60439-4858, United States*

³*Department of Chemistry, Faculty of Science, King Abdulaziz University, Jeddah 21589, Saudi Arabia*

[†]*A. E. P.-P. current address: Department of Inorganic Chemistry, Universidad Autónoma de Madrid, 28049 Madrid, Spain.*

*Corresponding Authors' Email: o-farha@northwestern.edu, j-hupp@northwestern.edu

Table of Contents

Materials	3
Physical Methods and Instrumentation	3
Syntheses	4
Single-Crystal X-Ray Crystallography	4
Difference Envelope Density Analyses	5
Gas Phase Catalysis	5
Table S1: Incorporation of NDC ligand with various loading conditions. All samples were submerged in the appropriate amount of DMF and heated for 16 h at 65 °C.	6
Figure S1: Representative ¹ H-NMR spectra of NU-1000 (red), NDC-SALI (blue), and NDC-SALI-HCl (purple) after digestion in a D ₂ SO ₄ /DMSO solution. Peaks used for quantification of NDC ligand are shown.	6
Table S2: Starting and ending NDC loading after an HCl wash of NDC-SALI.	6
Figure S2: (a) DRIFTS spectra of NU-1000 (red), NDC-SALI (blue), and NDC-SALI-HCl (purple) emphasizing the (b) –OH and (c) –C=O regions.	7
Figure S3: (a) Nitrogen isotherm and (b) DFT-calculated pore size distribution of NU-1000 (red), NDC-SALI (blue), and NDC-SALI-HCl (purple) taken at 77 K.	7
Table S3: Crystal data for NDC-SALI-HCl.	8
Figure S4: (a) SEM image and (b) corresponding energy dispersive line scan of a crystal of Co-SIM-NDC-SALI showing uniform deposition of Co throughout the crystal.	9
Figure S5: (a) Gravimetric nitrogen isotherms and (b) DFT-calculated pore size distribution of NDC-SALI-HC (red), Co-SIM-NDC-SALI (blue), and Co-SIM (purple) taken at 77 K. Calculated BET surface areas of the materials are 2030, 1730, and 1730 cm ² /g for NDC-SALI-HCl, Co-SIM-NDC-SALI, and Co-SIM, respectively.	9
Figure S6: (a) Volumetric nitrogen isotherms and (b) DFT-calculated pore size distribution of NU-1000 (red), Co-SIM-NDC-SALI (blue), and Co-SIM (purple) taken at 77 K. Calculated BET surface areas of the materials are 1150 and 1120 cm ² /cm ³ for NDC-SALI-HCl and Co-SIM-NDC-SALI, respectively.	10
Table S4: A summary of the BET surface area, pore volume (calculated using a DFT model), and highest uptake for the studied materials.	10
Figure S7: PXRD patterns of NU-1000 (red), NDC-SALI (blue), and Co-SIM-NDC-SALI (purple).	11
Figure S8: TGA curve of NU-1000 (red), NDC-SALI (blue), and Co-SIM-NDC-SALI (purple) under a flow of N ₂	11
Figure S9: DR-UV-VIS-NIR spectra of NU-1000 (red), Co-SIM-NDC-SALI (blue) and Co-SIM (purple).	12
Table S5: Summary of peaks observed in DR-UV-NIR spectra and their comparison to tetrahedral and octahedral Co ²⁺ complexes.	12
Figure S10: Post-catalysis characterization of Co-SIM-NDC-SALI including (a) N ₂ isotherm at 77 K, (b) PXRD pattern, (c) SEM image and (d) corresponding EDS line scan.	13
References:	13

Materials

Zirconyl chloride octahydrate, 1,3,6,8-tetrabromopyrene, (4-(methoxycarbonyl)phenyl)boronic acid, K_3PO_4 , tetrakis(triphenylphosphine) palladium(0), 2,6-naphthalenedicarboxylic acid (NDC), trifluoroacetic acid, benzoic acid, hydrochloric acid, hydrogen peroxide, high purity silica, cobalt and zirconium ICP standards were purchased from Sigma Aldrich Chemicals Company, Inc. (Milwaukee, WI) and were used as received. The ligand for NU-1000, 1,3,6,8-tetrakis(*p*-benzoic acid)pyrene (H_4TBAPy), was synthesized by a published procedure¹ and its purity was confirmed by 1H -NMR spectroscopy. Concentrated sulfuric acid was purchased from VWR Scientific, LLC (Chicago, IL). Acetone, chloroform, 1,4-dioxane, *N,N*-dimethylformamide (DMF), tetrahydrofuran (THF) and zirconium chloride were obtained from Fisher Scientific and used without further purification. Cobalt(II) acetate tetrahydrate (99.999% metal basis) was purchased from Alfa Aesar. Diethylformamide was purchased from TCI. Ultrapure deionized water (18.2 MB \cdot cm resistivity) was obtained from a Millipore Milli-Q Biocel A10 instrument (Millipore Inc., Billerica, MA).

All gases used for the adsorption and desorption measurements were Ultra High Purity Grade 5, and all other gases, were obtained from Airgas Specialty Gases (Chicago, IL).

Physical Methods and Instrumentation

N_2 isotherms were collected on a Micromeritics Tristar II 3020 instrument at 77 K. Pore-size distributions were calculated from these isotherms using a carbon split-pore model with a N_2 kernel.

Diffuse reflectance infrared Fourier transform spectra (DRIFTS) were recorded on a Nicolet 7600 FT-IR spectrometer equipped with an MCT/A detector. Samples diluted in KBr were measured with a KBr background. The spectra were collected at 1 cm^{-1} resolution and 128 scans were averaged over the spectral window of 675–4000 cm^{-1} .

Diffuse reflectance ultraviolet-visible-near infrared (DR-UV-NIR) spectra were measured on a Shimadzu UV-3600 equipped with a Harrick Praying Mantis diffuse reflectance accessory with polytetrafluoroethylene powder used as a baseline measurement. Measurements were made within the 200–1600 nm spectral window.

Powder X-ray diffraction (PXRD) patterns were collected on an ATX-G (Rigaku) instrument equipped with an 18 kW copper rotating anode x-ray source. Roughly 10 mg of sample was loaded onto a powder sample holder and mounted on the instrument. Samples were recorded from $1.5 < 2\theta < 20^\circ$ at a scan rate of $2^\circ/min$ and a step size of 0.05° .

Inductively coupled plasma–atomic emission spectroscopy data were collected on Varian Vista-MDX model ICP-AES spectrometer. Generally, the MOF sample was digested in 1.0 mL nitric acid and 0.25 mL 30% H_2O_2 followed by heating in a Biotage SPX microwave reactor at 150 $^\circ C$ for 5 min. This solution was then diluted with MilliQ water to a final volume of 15 mL.

Samples were digested with 5 drops of D_2SO_4 and diluted with $DMSO-d_6$ for 1H -NMR spectra.

Scanning electron microscopy (SEM) images were collected on a Hitachi SU8030 FE-SEM microscope with a field emission gun. Samples were coated with OsO₄ at ~7 nm of thickness with a Denton Desk III TSC Sputter Coater.

Thermal gravimetric analyses were conducted on a TA Instruments Q500. Samples (~3 mg) were placed in an aluminum pan and heated under N₂ gas flow to 600 °C at a rate of 10 °C/min.

Syntheses

NU-1000

NU-1000 was synthesized, HCl treated, and thermally activated as previously described unless mentioned otherwise.¹ Suitably sized crystals for single crystal x-ray diffraction studies were synthesized using a modified method. In short, ZrCl₄ (70 mg, 0.30 mmol) and benzoic acid (2 g, 16 mmol) were dissolved in 6 mL diethylformamide (DEF) and heated for 1 h at 100 °C. H₄TBAPy (40 mg, 0.059 mmol) was dissolved in 4 mL DEF and heated for 1 h at 100 °C. The vials were removed from the oven and cooled to room temperature before being mixed together. The resultant solution was heated at 120 °C for 48 h. The sample was subsequently acid activated using a previously described method.²

NDC-SALI-HCl

NDC (79 mg, 0.37 mmol) was dissolved in 10 mL DMF in an 8-dram vial with sonication. NU-1000 (200 mg, 0.091 mmol) was added to the solution and heated overnight (16 h) at 65 °C. The resultant material was washed with hot DMF four times over 8 h. The material was then transferred to a 100-mL screw-top jar with 48 mL DMF. Then, 2 mL of aqueous 8 M HCl was added and the jar was placed into a 100 °C oven overnight. The material was then washed with DMF over the course of 8 h (4 × 40 mL) and then solvent exchanged to acetone (4 × 40 mL) before thermally activating the material at 100 °C for 16 h under dynamic vacuum.

NDC-SALI-HCl - Single Crystal

An identical procedure as described above was used to load NDC ligands in crystals large enough for single crystal diffraction experiments. Samples were HCl treated but kept in dimethylformamide and not thermally evacuated before single crystal diffraction data was collected.

Co-SIM-NDC-SALI

Cobalt acetate tetrahydrate (125 mg, 0.50 mmol) was dissolved in 18.7 mL DMF with sonication. Subsequently, NDC-SALI-HCl (150 mg, 0.063 mmol) was added to the solution and placed in a 100 °C oven for 16 h. The material was centrifuged and washed with hot DMF (4 × 40 mL) before being solvent exchanged to acetone (4 × 40 mL). The material was then thermally treated at 100 °C for 16 h under dynamic vacuum.

Single-Crystal X-Ray Crystallography.

X-ray crystal structure analysis was carried out using a Bruker Kappa APEX II CCD detector equipped Cu K α (λ = 1.54178 Å) microsource with MX optics. A single crystal was mounted on

MicroMesh (MiTeGen) with paratone oil. The structure was solved by direct methods (SHELXS-97),³ and refined by full-matrix least-squares refinement on F^2 (SHELXL-2017/1)⁴ using the Yadokari-XG software package.⁵ Some thermal parameter restraints (RIGU, SIMU, ISOR) were used in the refinements on TBAPy and NDC linkers. The disordered non-coordinated solvents were removed using the PLATON SQUEEZE program.⁶ The refinement result is summarized in Table S3. Crystallographic data in CIF format have been deposited in the Cambridge Crystallographic Data Centre (CCDC) under deposition number CCDC-1580358. The data can be obtained free of charge via www.ccdc.cam.ac.uk/data_request/cif (or from the Cambridge Crystallographic Data Centre, 12 Union Road, Cambridge CB2 1EZ, U.K.).

Difference Envelope Density Analyses

Synchrotron powder X-ray diffraction (PXRD) data were collected at beamline 17-BM at the Advanced Photon Source (APS) at Argonne National Laboratory (ANL). The incident X-ray wavelength was 0.45336 Å. Data were collected using a Perkin Elmer flat panel area detector (XRD 1621 CN3/EHS) over the angular range 0.5–10° 2-theta. Samples were carefully ground and loaded into 1 mm diameter kapton capillaries. All measurements were performed at room temperature and ambient pressure. Sample-detector distance, beam center, detector tilt and rotation, and angular corrections were determined via calibration with NAC (Na₂Ca₃Al₂F₁₄) in GSAS-II.⁷ Lattice parameters and Bragg scattering intensities of reflections out to 2-theta=10° were extracted *via* Le Bail whole pattern fitting of the previously reported NU-1000 crystal structure to diffraction data.^{2,8,9} Structure envelopes (SEs) encompassing regions of high electron density were generated from extracted peak intensities as previously described.^{10,11} To isolate contributions from species added during deposition, difference envelope densities (DEDs) were calculated *via* subtraction of the SE of the parent material from those of metalated MOFs.

Gas Phase Catalysis

Catalyst activity and selectivity measurements were recorded using a packed-bed flow reactor (Microactivity Efficient, MAE). Using an Agilent 7890A GC system, the amount of propane and propene were analyzed by an FID detector using an Agilent J&W GC column (GS-Alumina, 30 m × 0.535 mm); the amount of CO₂ and CO is determined by a TCD detector using a combination of two columns (Column 1: HP-Plot Q, Column 2: HP-Plot Molesieve). The amounts of the gases were determined based on the integration areas converted to mol% using relevant calibration curves.

The gases used for gas-phase oxidative dehydrogenation of propane catalysis were 3% propane balanced with He and 10% O₂ balanced with He.

Table S1: Incorporation of NDC ligand with various loading conditions. All samples were submerged in the appropriate amount of DMF and heated for 16 h at 65 °C.

NDC Equivalents Added	Concentration (M)	NDC Incorporated (per Zr ₆)
1	0.07	0.99
2	0.07	1.42
4	0.07	2.5
4	0.07	2.25
8	0.07	2.63
2	0.035	1.65
4	0.035	2.44

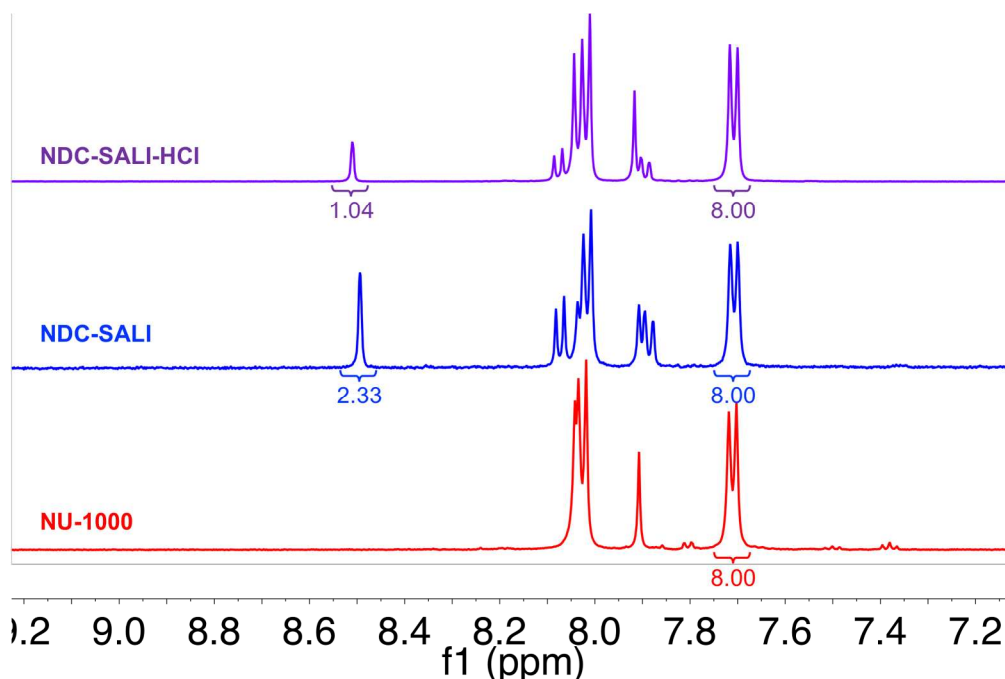


Figure S1: Representative ¹H-NMR spectra of NU-1000 (red), NDC-SALI (blue), and NDC-SALI-HCl (purple) after digestion in a D₂SO₄/DMSO solution. Peaks used for quantification of NDC ligand are shown.

Table S2: Starting and ending NDC loading after an HCl wash of NDC-SALI.

Starting NDC Incorporated (per Zr ₆)	Concentration of HCl added (M)	Temperature (°C)	Ending NDC Incorporated (per Zr ₆)
2.63	0.1	20	1.83
2.63	0.1	100	2.04
2.63	1	100	1.67
2.63	8	80	1.15
2.5	8	100	1.04

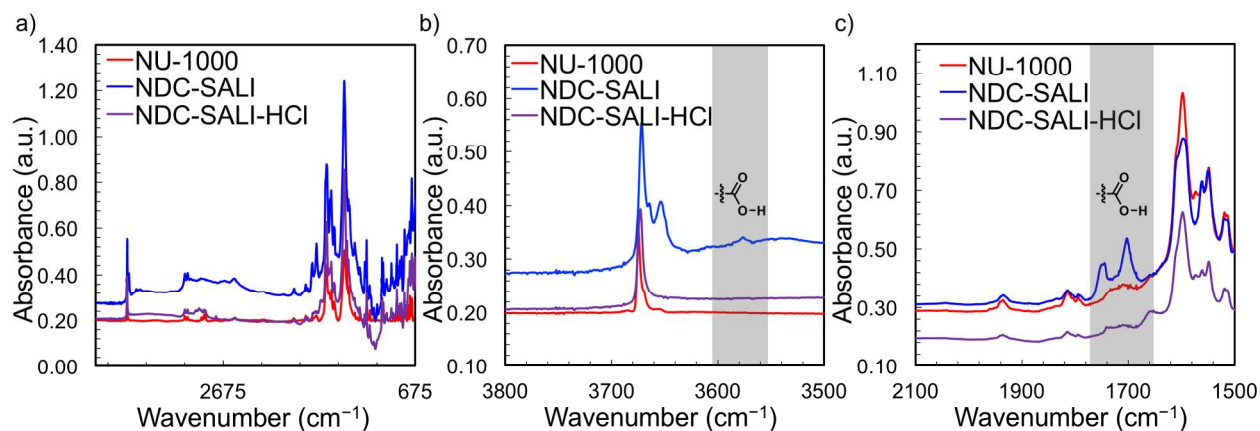


Figure S2: (a) DRIFTS spectra of NU-1000 (red), NDC-SALI (blue), and NDC-SALI-HCl (purple) emphasizing the (b) –OH and (c) –C=O regions.

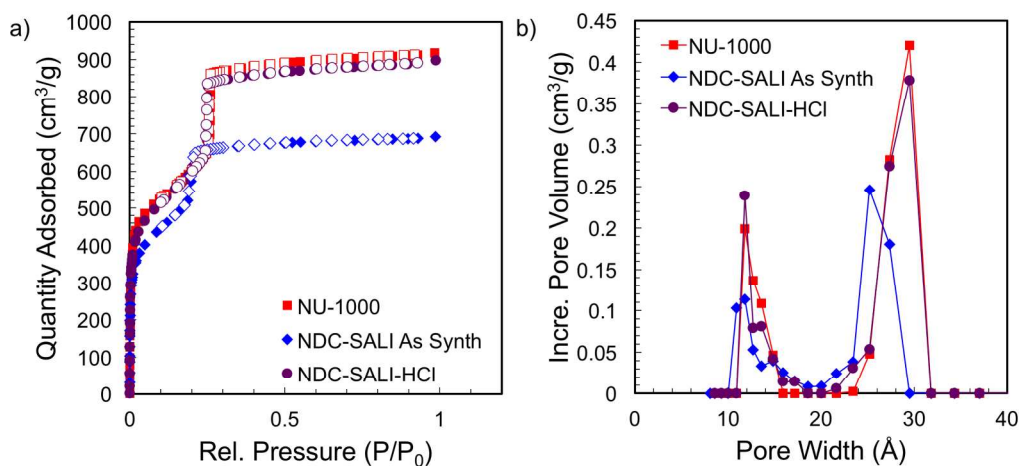


Figure S3: (a) Nitrogen isotherm and (b) DFT-calculated pore size distribution of NU-1000 (red), NDC-SALI (blue), and NDC-SALI-HCl (purple) taken at 77 K.

Table S3: Crystal data for NDC-SALI-HCl

Empirical Formula	C ₁₀₀ H ₆₀ O ₃₈ Zr ₆
Formula Weight (g/mol)	2454.9
Temperature (K)	100
Wavelength (Å)	1.54178
Crystal System	hexagonal
Space Group	<i>P</i> 6/ <i>mmm</i> (no.191)
Unit Cell Dimensions (Å)	<i>a</i> = 38.926(3)
	<i>b</i> = 38.926(3)
	<i>c</i> = 16.835(2)
Volume (Å ³)	22091 (4)
<i>Z</i>	3
Calc'd Density (g/cm ³)	0.533 cm ³ /g
μ (mm ⁻¹)	1.933
<i>F</i> (000)	3432
Crystal Size (mm ³)	0.05 × 0.03 × 0.03
θ_{min} , θ_{max} (°)	3.7, 58.0
Reflections Collected	43388
Independent Reflections	5758
<i>R</i> _{int}	0.1996
Goodness-of-fit on <i>F</i> ²	1.253
<i>R</i> ₁ [<i>I</i> > 2σ(<i>I</i>)]	0.1246
<i>wR</i> ₂ [all data]	0.3424
CCDC number	CCDC-1580358

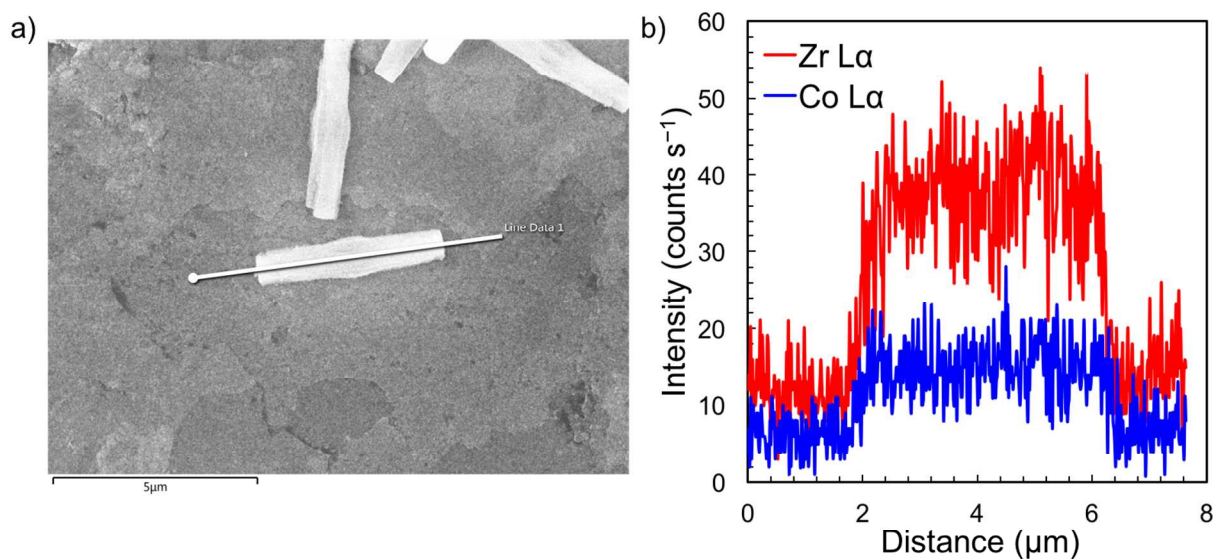


Figure S4: (a) SEM image and (b) corresponding energy dispersive line scan of a crystal of Co-SIM-NDC-SALI showing uniform deposition of Co throughout the crystal.

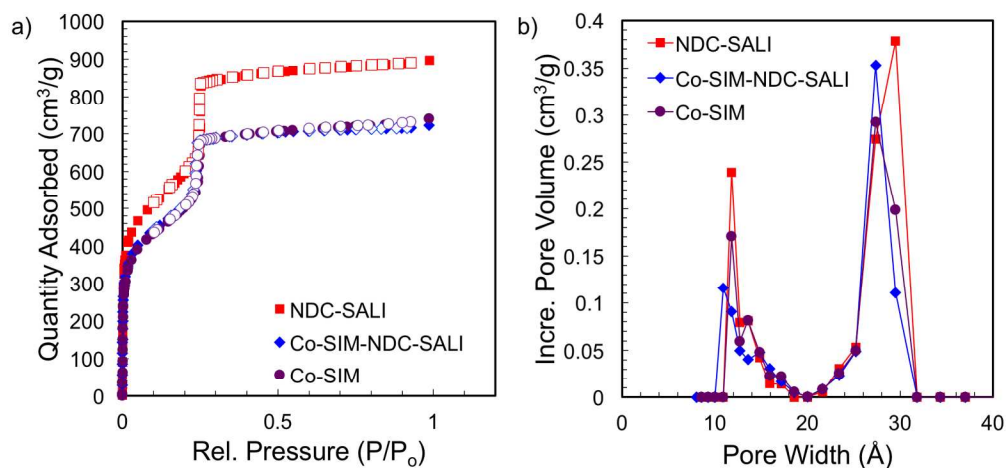


Figure S5: (a) Gravimetric nitrogen isotherms and (b) DFT-calculated pore size distribution of NDC-SALI-HC (red), Co-SIM-NDC-SALI (blue), and Co-SIM (purple) taken at 77 K. Calculated BET surface areas of the materials are 2030, 1730, and 1730 cm^2/g for NDC-SALI-HCl, Co-SIM-NDC-SALI, and Co-SIM, respectively.

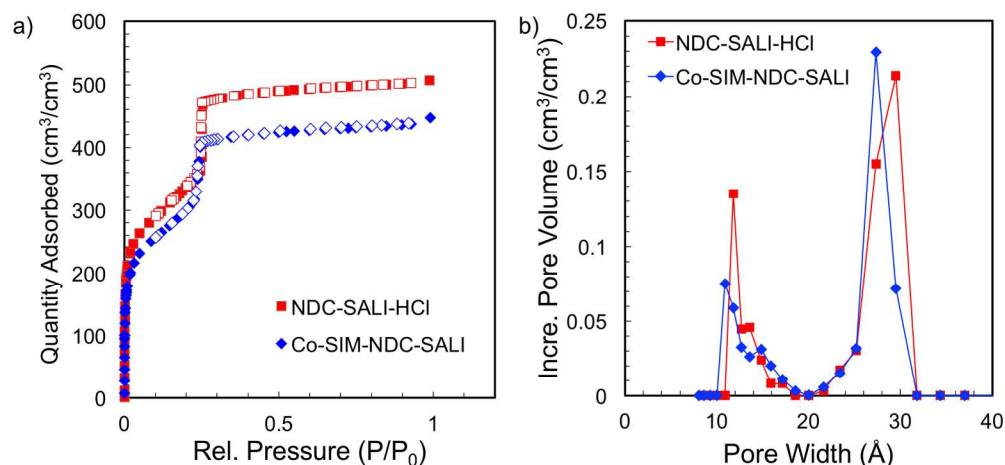


Figure S6: (a) Volumetric nitrogen isotherms and (b) DFT-calculated pore size distribution of NU-1000 (red), Co-SIM-NDC-SALI (blue), and Co-SIM (purple) taken at 77 K. Calculated BET surface areas of the materials are 1150 and 1120 cm²/cm³ for NDC-SALI-HCl and Co-SIM-NDC-SALI, respectively.

Table S4: A summary of the BET surface area, pore volume (calculated using a DFT model), and highest uptake for the studied materials

Material	BET Surface Area (m ² /g)	Pore Volume (cm ³ /g)	Highest Uptake (cm ³ /g)
NU-1000	2100	1.24	917
NDC-SALI	1720	0.93	690
NDC-SALI-HCl	2030	1.21	900
Co-SIM	1700	1.00	740
Co-SIM-NDC-SALI	1730	0.98	720

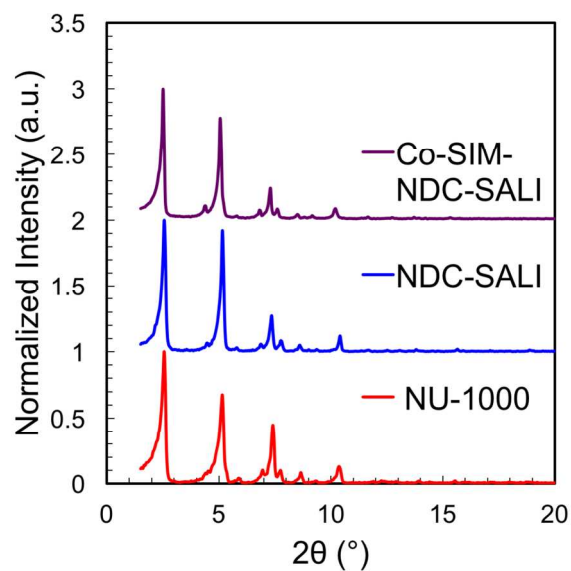


Figure S7: PXRD patterns of NU-1000 (red), NDC-SALI (blue), and Co-SIM-NDC-SALI (purple)

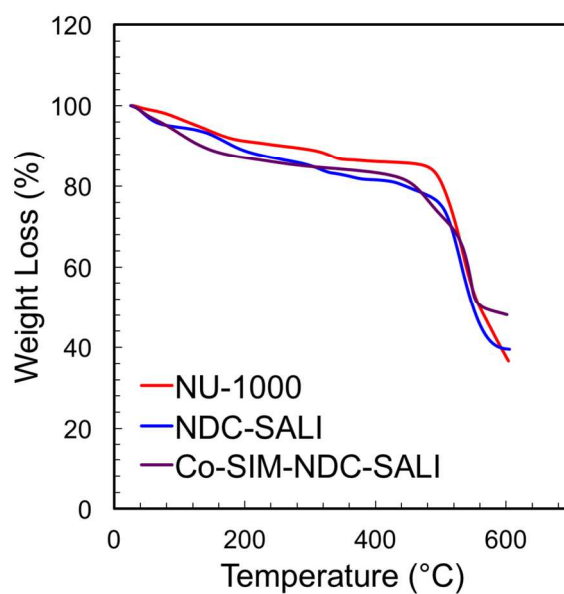


Figure S8: TGA curve of NU-1000 (red), NDC-SALI (blue), and Co-SIM-NDC-SALI (purple) under a flow of N_2 .

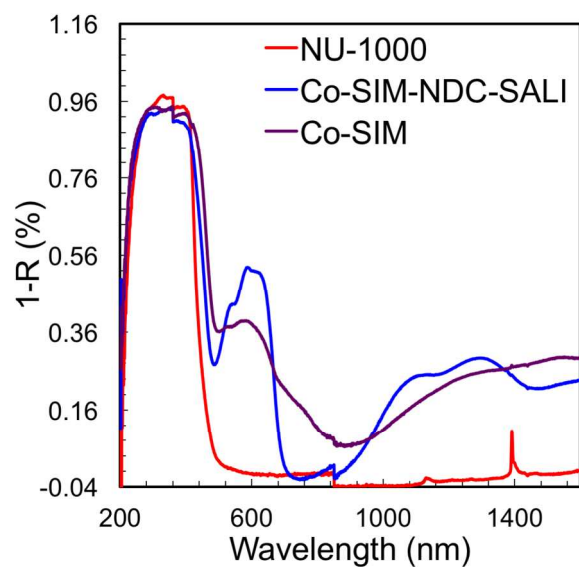


Figure S9: DR-UV-VIS-NIR spectra of NU-1000 (red), Co-SIM-NDC-SALI (blue) and Co-SIM (purple).

Table S5: Summary of peaks observed in DR-UV-NIR spectra and their comparison to tetrahedral and octahedral Co^{2+} complexes.

Material	Wavelength (nm)					
Co-SIM-NDC-SALI	536	584	615	1079	1284	
Co-SIM	519	580	747	1245	1500	
$\text{Co}^{2+} \text{ T}_d^{12}$	537	590	647	1000–1400		
$\text{Co}^{2+} \text{ O}_h^{12}$	500	526	588	625	730	1000–1400

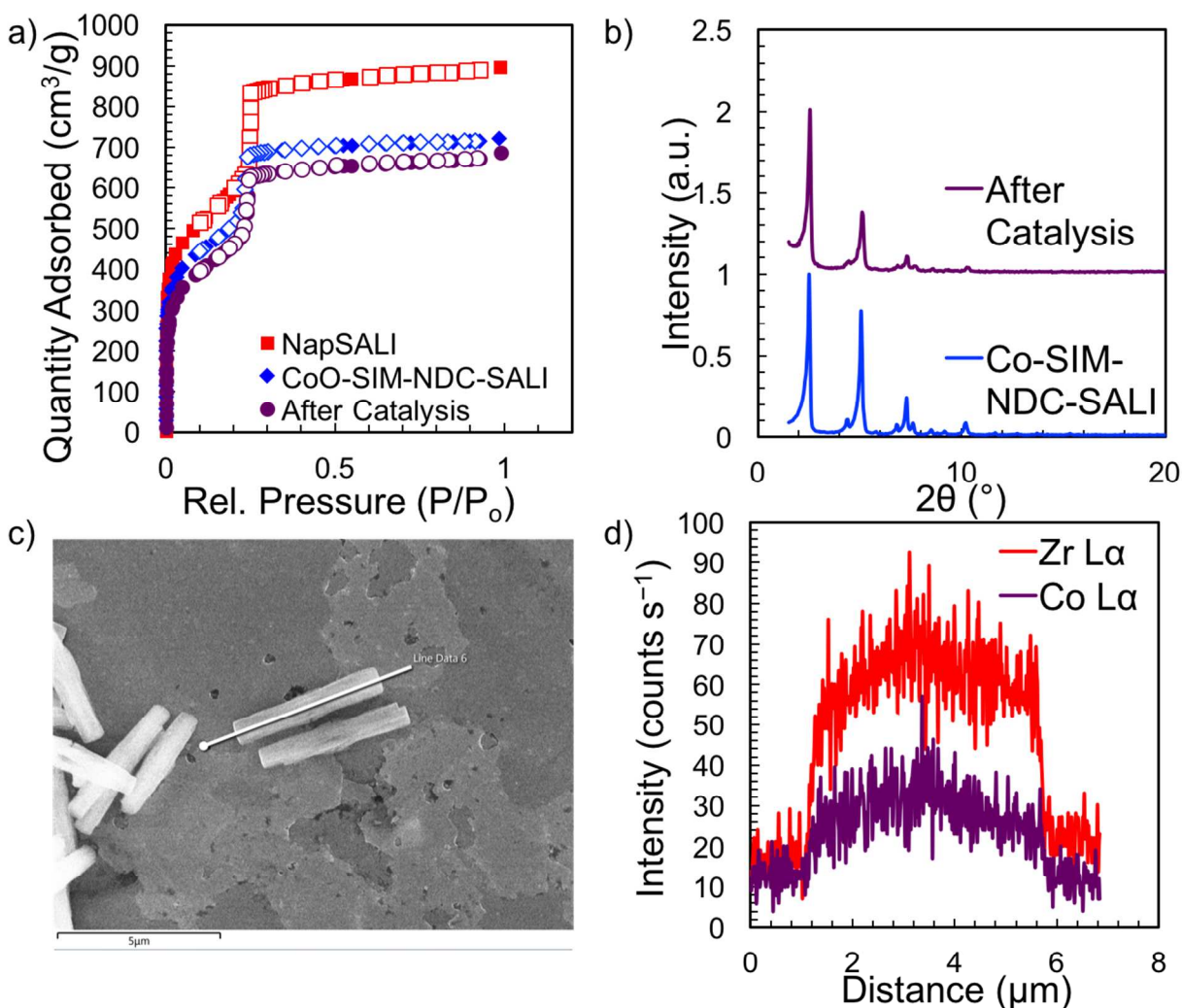


Figure S10: Post-catalysis characterization of Co-SIM-NDC-SALI including (a) N₂ isotherm at 77 K, (b) PXRD pattern, (c) SEM image and (d) corresponding EDS line scan.

References:

- (1) Wang, T. C.; Vermeulen, N. A.; Kim, I. S.; Martinson, A. B. F.; Stoddart, J. F.; Hupp, J. T.; Farha, O. K. Scalable Synthesis and Post-Modification of a Mesoporous Metal-Organic Framework Called NU-1000. *Nat. Protoc.* **2016**, *11*, 149-162.
- (2) Mondloch, J. E.; Bury, W.; Fairen-Jimenez, D.; Kwon, S.; DeMarco, E. J.; Weston, M. H.; Sarjeant, A. A.; Nguyen, S. T.; Stair, P. C.; Snurr, R. Q.; Farha, O. K.; Hupp, J. T. Vapor-Phase Metalation by Atomic Layer Deposition in a Metal–Organic Framework. *J. Am. Chem. Soc.* **2013**, *135*, 10294-10297.
- (3) G. M. Sheldrick. SHELX97 Programs for Crystal Structure Analysis; University of Göttingen: Göttingen, Germany, 1998
- (4) Sheldrick, G. Crystal structure refinement with SHELXL. *Acta Cryst. C* **2015**, *71*, 3-8.

- (5) Kabuto, C.; Akine, S.; Kwon, E. Release of Software (Yadokari-XG 2009) for Crystal Structure Analyses. *J. Cryst. Soc. Jpn.* **2009**, *51*, 218-224.
- (6) Spek, A. Structure validation in chemical crystallography. *Acta Cryst. D* **2009**, *65*, 148-155.
- (7) Toby, B. H.; Von Dreele, R. B. GSAS-II: the genesis of a modern open-source all purpose crystallography software package. *J. Appl. Crystallogr.* **2013**, *46*, 544-549.
- (8) Le Bail, A. Whole powder pattern decomposition methods and applications: A retrospection. *Powder Diffr.* **2012**, *20*, 316-326.
- (9) Petříček, V.; Dušek, M.; Palatinus, L. Crystallographic Computing System JANA2006: General features. *Zeitschrift für Kristallographie - Crystalline Materials* **2014**, *229*, 345.
- (10) Yakovenko, A. A.; Reibenspies, J. H.; Bhuvanesh, N.; Zhou, H.-C. Generation and applications of structure envelopes for porous metal-organic frameworks. *J. Appl. Crystallogr.* **2013**, *46*, 346-353.
- (11) Yakovenko, A. A.; Wei, Z.; Wriedt, M.; Li, J.-R.; Halder, G. J.; Zhou, H.-C. Study of Guest Molecules in Metal–Organic Frameworks by Powder X-ray Diffraction: Analysis of Difference Envelope Density. *Cryst. Growth Des.* **2014**, *14*, 5397-5407.
- (12) Fierro, G.; Eberhardt, M. A.; Houalla, M.; Hercules, D. M.; Hall, W. K. Redox Chemistry of CoZSM-5 Zeolite. *J. Phys. Chem.* **1996**, *100*, 8468-8477.